Pflügers Arch – Eur J Physiol (2000) 439:829–837
Digital Object Identifier (DOI) 10.1007/s004249900233

ORIGINAL ARTICLE

J.O. Bustamante · E.R.F. Michelette · J.P. Geibel
J.A. Hanover · T.J. McDonnell · D.A. Dean

Dendrimer-assisted patch-clamp sizing of nuclear pores

Received:11 October 1999 / Received after revision and accepted: 7 December 1999 / Published online: 27 January 2000

Abstract Macromolecular translocation (MMT) across the nuclear envelope (NE) occurs exclusively through the nuclear pore complex (NPC). Therefore, the diameter of the NPC aqueous/electrolytic channel (NPCC) is important for cellular structure and function. The NPCC diameter was previously determined to be ≅10 nm with electron microscopy (EM) using the translocation of colloidal gold particles. Here we present patch-clamp and fluorescence microscopy data from adult cardiomyocyte nuclei that demonstrate the use of patch-clamp for assessing NPCC diameter. Fluorescence microscopy with B-phycoerythrin (BPE, 240 kDa) conjugated to a nuclear localization signal (NLS) demonstrated that these nuclei were competent for NPC-mediated MMT (NPC-MMT). Furthermore, when exposed to an appropriate cell lysate, the nuclei expressed enhanced green fluorescence protein (EGFP) after 5–10 h of incubation with the plasmid for this protein (pEGFP, 3.1 MDa). Nucleus-attached patch-clamp showed that colloidal gold particles were not useful probes; they modified NPCC gating. As a result of this finding, we searched for an inert class of particles that could be used without irreversibly affecting NPCC gating and found that fluorescently labeled Starburst dendrimers, a distinct class of polymers, were useful. Our patch-clamp and fluorescence microscopy data with calibrated dendrimers indicate that the cardiomyocyte NPCC diameter varies between 8 and 9 nm. These studies open a new direction in the investigation of live, continuous NPC dynamics under physiological conditions.

Key words Cardiac myocytes · Cell nucleus · Dendrimers · EGFP · Gene activity · Gene expression · Ion channels · Nuclear ion channels · Nuclear pores · Nucleocytoplasmic transport · Patch-clamp · pEGFP · Pore diameter

Abbreviations *EM*: Electron microscopy · *NPC*: nuclear pore complex · *NPCC*: NPC channel · γ: ion conductance · p_o: open channel probability – probability of finding the channel open · Γ_p: patch ion conductance · I_p: patch ion current · V_p: patch voltage; ≅: in the order of – meaning the closest numerical representation in base 10 (e.g., 10^2 is the order of a value of 82) · ≈: approximately equal (e.g., 82.15≈82.22)

J.O. Bustamante (✉) · E.R.F. Michelette
The Nuclear Physiology Laboratory, Universidade Tiradentes,
Rua B-508, Praia Aruana, Aracaju, Sergipe 49030–270, Brazil1
URL: http://www.geocities.com/TheTropics/6066/index.html,
e-mail: jobustamante@mcafeemail.com,
Tel.: +55-79-988-4320, Fax: +55-79-2433661)

J.O. Bustamante
Dept. Medicine, Yale University School of Medicine, New Haven, CT 06520, USA

J.O. Bustamante · J.P. Geibel
Dept. Surgery, Yale University School of Medicine, New Haven, CT 06520, USA

J.P. Geibel
Dept. Cellular and Molecular Physiology,
Yale University School of Medicine, New Haven, CT 06520, USA

J.A. Hanover
Lab. Cell Biochemistry, NIDDK, National Institutes of Health,
Bethesda, MD 20892–0850, USA

T.J. McDonnell
Dept. Molecular Pathology, The University of Texas,
M.D. Anderson Cancer Center, Houston, TX 77030, USA

D.A. Dean
Dept. Microbiology and Immunology,
University of South Alabama College of Medicine, Mobile,
AL 36688–0002, USA

Introduction

Electron microscopy (EM) studies with colloidal gold particles indicate that the diameter of the nuclear pore complex (NPC) aqueous/electrolytic channel (NPCC) is ≅10 nm (e.g., [1, 2, 3]). On the basis of the reported NPC geometry and electrical conductivity of the medium, the predicted ion conductance (γ) for a single NPC channel (NPCC) is ≅10^2–10^3 pS (e.g., [4]). The NPCC passive diameter changes (e.g., 20–70 kDa, 3–12 nm) with cell

type and the phase of the cell cycle (e.g., [2]). In contrast, during macromolecular translocation (MMT), the NPC of any cell displays a larger, labile diameter that accommodates macromolecules, or complexes thereof, as massive as ribonucleoprotein particles (RNPs), RNAs and DNAs (e.g., [5]). The requirements for MMT depend on the nature of the translocating particle or cargo. The cargo must contain a nuclear localization signal (NLS), a nuclear export signal (NES), or both, and its translocation is dependent upon a gradient of Ran-GDP/GTP, ATP, cargo receptors (importins or exportins that form the translocating complex), etc. (e.g., [2, 3, 4, 5]).

Calculation of pore diameter and diffusional constants assumes that the NPCC is always open. However, patch-clamp investigations indicate that the NPC behaves like an ion channel (e.g., [6, 7], see [4]), with gates opening and closing in a probabilistic manner (e.g., [8]). Patch-clamp demonstrates that, despite the large NPCC diameter, the NPC gate(s) is(are) sufficient to regulate ion flow into and out of the nucleus through changes in its open probability (see [4]). Open–close channel gating as well as channel plugging (e.g., [6, 9, 10, 11]) explain why it is possible to observe significant ion gradients across the nuclear envelope (NE) and thus nuclear ion regulation (e.g., [12]). The phenomenon of ion channel plugging has been proposed for endoplasmic reticulum (ER) protein-conducting channels (e.g., [9]) and mitochondrial channels (e.g., [13, 14, 15]). Plugging of the NPC diffusional channel was considered more than a decade ago to explain fluorescence microscopy observations (page 350 in [16]) and the concept seems to have regained recognition in this field (e.g., [12, 17, 18]).

A logical continuation of our patch-clamp studies (e.g., [6, 8, 19, 20, 21]) would be to attempt to incorporate the EM method of pore sizing with direct measurements of the NPCC electrical conductance, γ, using patch-clamp. As previously explained [10], the central idea of using particles of known diameter to size a membrane channel with electrical methods is similar to the resistive pulse principle of Coulter counters and other technologies. Briefly, each time non-conducting particles translocate through the lumen of the electrolyte-filled aqueous channel or pore, γ (determined by electrolyte aqueous composition and channel geometry) decreases (discussed in Appendix I). The reduction in γ is directly related to the particle size and its concentration as predicted by the restricted-diffusion theory (e.g., [10]). Consequently, NPCC diameter for passive diffusion corresponds to the minimal diameter of a non-conducting, inert particle that would interrupt ion flow along the channel or pore.

It is not clear whether colloidal gold particles may act as non-conductors or charge carriers and, thus, whether our macromolecule-conducting ion channel model is applicable (e.g., [6]). Since colloidal gold irreversibly alters NPCC gating in our preparation, we searched for inert substitutes and found that calibrated dendrimers called Starburst (Dendritech, Midland, Mich., USA; e.g., [22]) were suitable for assessing the NPCC diameter. Starburst dendrimers are hydrophilic, monodisperse, highly branched macromolecules and their unique synthesis process yields particles of controlled diameter and molecular weight (e.g., [22]). Amino- and carboxyl-terminated Starburst dendrimer microparticles are commercially available and, as dielectric, tractable with current theory for polymer-conducting ion channels [10]. As we show here, an added advantage of using these dendrimer particles is that they may be coupled with fluorescent markers such as fluorescein isothiocyanate (FITC). Consequently, their ability to translocate along the NPCC can be independently determined using fluorescence microscopy.

We have proposed that the large-γ channel activity recorded with patch-clamp from the NE of cardiac myocytes corresponds to ion flow along the NPCC (e.g., [6, 20, 21]). Here we show with patch-clamp that colloidal gold particles modify NPCC gating in these isolated nuclei and, thus, that they are not reliable for NPCC diameter determination. However, we show that calibrated dendrimers can reliably be used to measure NPCC diameter. Our estimates suggest that this diameter is between 8 and 9 nm (80 and 90 Å) for quiescent adult cardiac myocytes. Our results support the use of patch-clamp for sizing the NPCC diameter.

Materials and methods

Nuclei isolation

To ensure that the isolated nuclei remained in a medium with composition close to that of their native environment, we modified the methods previously reported for cardiac myocyte nuclei isolation [6, 8, 19]. A total of 82 male Swiss-Webster mice (20–22 g) were used. Each mouse was decapitated and its beating heart was excised and washed with Ca^{2+}-, Mg^{2+}-free saline (mM: 150 NaCl, 10 Hepes, 5 KOH; pH 7.2–7.3, room temperature). The pieces of tissue were then placed in ice-cold, Ca^{2+}-, Mg^{2+}-free saline (mM: 150 KCl, 10 HEPES, 5 KOH; pH 7.2) and cut with sharp scissors (SuperCut; Biomedical Research Instruments, Rockville, Md., USA) into small 2- to 3-mm pieces and washed for 5 min in this solution. The saline was then replaced with an ice-cold high-K-EGTA solution (mM: 135 KCl, 5 EGTA, 5 $MgCl_2$, 10 HEPES, and 15 KOH, pH 7.2). The pieces of tissue, along with 5 ml of this solution, were placed in an ice-cold Dounce manual tissue grinder (Wheaton-33 low extractable borosilicate glass; Wheaton, Millville, N.J., USA). Nuclei were released by four to six strokes with the loose-fitting pestle of the tissue grinder. Rather than purifying the nuclei through a Percoll gradient as previously described [19], we used a graded series of nylon gauze (100, 50, 25 and 10 µm sieving capacity). The procedure ensured that the isolated nuclei remained in their natural cytosol (albeit modified by the high-K-EGTA medium).

Solutions and chemical reagents

Salt solutions were prepared from pre-tested reagents (Molecular Biology Grade, Sigma). A high-K saline solution (mM: 150 KCl, 5 $MgCl_2$, 10 HEPES, and 4 KOH; pH 7.2–7.3) was used as the control solution for both pipette and bath. These solutions were filtered at 0.2 µm. Colloidal gold (5 and 20 nm diameter) and amino-terminated Starburst dendrimer particles (5.4 and 8.4 nm diameter) were obtained from Polysciences (Warrington, Pa., USA).

These substances were supplied fresh from the source and without preservatives. Stock and test solutions were prepared and stored in ice-cold high-K saline in less than 5 min prior to use. Starburst dendrimer particles of 5.4 and 8.4 nm diameter were selected as they could also be purchased with FITC conjugated to them (Polysciences). Particles of other sizes were too big or too small for the calibration of NPCC diameter in our preparation. Liquid handling and storage were exercised with extreme caution to avoid artifacts resulting from particle and aerosol contamination. Biopur (Eppendorf, Hamburg, Germany) pipettes tips and opaque microcentrifuge tubes were used to prevent both organic and inorganic contamination. An aerosol-proof pipette with special pipette tips (Biomaster 4830, Eppendorf) was used for preparing the test solutions.

Patch clamp

Our procedures for patch-clamping isolated nuclei are described elsewhere [6, 8, 19]. Briefly, fiber-filled glass tubing (TW150F-4, World Precision Instruments, Sarasota, Fla., USA) was used to manufacture the patch-clamp pipettes. The pipettes were filled with either the high-K control solution or with the test solutions containing the particles of colloidal gold or dendrimers. The pipettes had a small intrinsic suction resulting from their internal capillary forces. However, to ensure that no particle tested (i.e., colloidal gold or dendrimer) escaped from the pipette and affected the NPCC, a small negative pressure (–5 mmHg) was applied prior to contact of the NE. As previously reported (e.g., 8, 19]), all applied voltages as well as acquisition and processing of the data was carried out with Axon Instruments instrumentation (Foster City, Calif., USA). Voltage values given in this paper are those applied to the glass pipette lumen. Since the resting potential of our preparation is negligible (see [8, 19]), the applied potential across the NE (*V*, given in mV throughout the paper) is equal to the inverse of the pipette potential ([8, 19] – see [4]). To avoid accumulating possible voltage-induced changes in channel gating (e.g., potential of inactivation, see [8]), small voltage steps (e.g., ±10 mV) were applied when possible. Higher voltage steps (e.g., ±40 mV) were used when the signals became too small to allow proper evaluation of the phenomena (e.g., during pore plugging by translocating particles). Thus, higher voltages served to increase the signal to noise ratio (i.e., to improve the relative cleanliness of the recording). We previously demonstrated that the single-channel conductance, γ, of open, unplugged pores is independent of voltage [8, 19]. Therefore, any voltage-dependent change should be considered an effect of the voltage on the translocating particle and not on the diameter of the pore. Experiments were timed from the moment of tight seal formation between the tip of the patch-clamp pipette and the outer surface of the NE (i.e., gigaseal or $>10^9$ ohms or Ω, and 1 Ω=1 Volt/Ampere). A small, 1-mV-amplitude pulse of 1 ms duration was applied to measure the gigaseal formation at the beginning of the experiment. This pulse was also used throughout the experiment to monitor the status of the pipette-membrane seal. Ensembles of eight patch ion conductance (Γ_p) traces were computed from the current record ensembles. Successive records in each ensemble were separated by 300-ms intervals at which the NE was held at 0 mV. Note that in our experiments the voltage is constant as it is clamped. Therefore, Γ_p is simply the recorded patch current, I_p, scaled down by the patch voltage, V_p (i.e., $\Gamma_p=I_p/V_p$). The signals were filtered at 100 Hz (8-pole Bessel filter – see [8, 19]).

Note that, in the presence of a tight gigaseal ($>10^9$ Ω), Γ_p is the sum of the individual contributions of the γ of each NPCC weighted by their open probability, p_o. Thus, for a NE patch consisting of identical channels, as appears to be in cardiac patches [8], the average patch conductance, $<\Gamma_p>$, is the sum of the single NPCC conductance, γ, weighed by their open probability, p_o, (i.e., $\langle \Gamma_p \rangle = \sum_{i=1}^{i=N} p_{o_i} \gamma_i$; where *i* represents the value for the *i*th channel of the patch). For a patch of *N* identical channels, $<\Gamma_p>=Np_o\gamma$. Thus, only when all the channels of the patch open simultaneously does the instantaneous value of Γ_p equal the number of ion-conducting channels times the single-channel conductance (i.e., $\Gamma_p=N\gamma$). For the sake of clarity, only selected ensembles are given to illustrate the highlights of the experiments. Both direct and indirect methods were use to calculate single NPC ion conductance, γ. The ion current flowing through a single NPC channel (Δi) was manually measured by calculating the difference between consecutive open-close and close-open channel levels discernible by their step-like nature typical of ion channel state transitions. We did not include slow changes in current as they do not represent true state transitions but suggest partial channel plugging. For single-trace inspection, measurement and analysis, we used the Fetchan module of pClamp (Axon Instruments). The value of γ was then calculated by dividing Δi by the amplitude of the applied voltage pulse. When this direct approach was not possible due to excessive intrinsic channel noise (caused by the translocating particles), the all-points amplitude histogram produced by Fetchan was used in conjunction with the module pStat of pClamp. The pStat module allowed the determination of the histogram peaks by multi-Gaussian fitting. The analysis used for the patch-clamp records is shown in Fig. 1 for control conditions. Figure 1A shows a sequence of eight I_p records (i.e., a record ensemble). The number at the top-left of each record shows the sequence order (i.e., 1 for the 1st record, 8 for the 8th). Figure 1B shows the all-points amplitude histogram for the whole I_p record ensemble. The continuous line forming the envelope of the histogram corresponds to the multi-Gaussian fitting and the continuous lines forming the envelope of individual peaks represent the simple Gaussian fitting for that particular peak. All the experiments were carried out on nucleus-attached patches. Under these conditions, the NPCs outside the pipette tip short-circuit the nucleoplasm with the external bath (held at 0 mV, the reference potential). Therefore, the voltage sensed by the NPCs inside the patch is the negative of the voltage applied to the interior of the pipette (see [4]). The major electrical charge carrier in this preparation is K^+ [8, 19]. Thus, the carriers will move outward (i.e., away from the nucleus) when a negative voltage is applied to the pipette lumen and inward when the applied voltage is positive. These pipette voltages are equivalent to a positive and negative voltage applied to the nucleoplasm. Positive and negative current means, respectively, outward and inward movement of ions (mainly K^+). The use of conductance (γ and Γ_p) to represent the ion channel activity eliminates the issue of directionality as it is always positive because both current and voltage have the same sign.

Fluorescence microscopy

We previously indicated that to validate the patch-clamp approach for the recording of NPC ion channel behavior, the nuclei used must demonstrate all the expected normal NPC transport properties (discussed in [4]). This is important because it has been recently shown that there is potential contamination with ER remains of the patched outer NE membrane [23]. Therefore, in order for us to demonstrate that the potential contribution of channels in the ER remains is not significant in our experiments (vis à vis that of NPCCs), we carried out the present fluorescence microscopy measurements to test the functionality of NPCs for passive and active transport.

NPC transport properties were independently studied in 12 mice with laser scanning confocal fluorescence microscopy (MRC-600, Bio-Rad, Hercules, Calif., USA; LSM 410, Carl Zeiss, Oberkochen) and with the fluorescence microscope used for patch-clamping ([24]; Bustamante, unpublished). In addition to using FITC-labeled Starburst dendrimers, we used FITC-labeled dextrans (1 μM, 4–150 kDa, Molecular Probes, Eugene, Ore., USA). NPCs' capacity for MMT was tested with 100 nM B-phycoerythrin (BPE, 240 kDa, Molecular Probes, Eugene, Ore., USA) conjugated to the NLS of the SV40 large T antigen (Sigma). The NLS-conjugated BPE (BPE+NLS) was applied in the presence of cell lysate supplemented with 1 μM Ca^{2+} and an ATP-regenerating

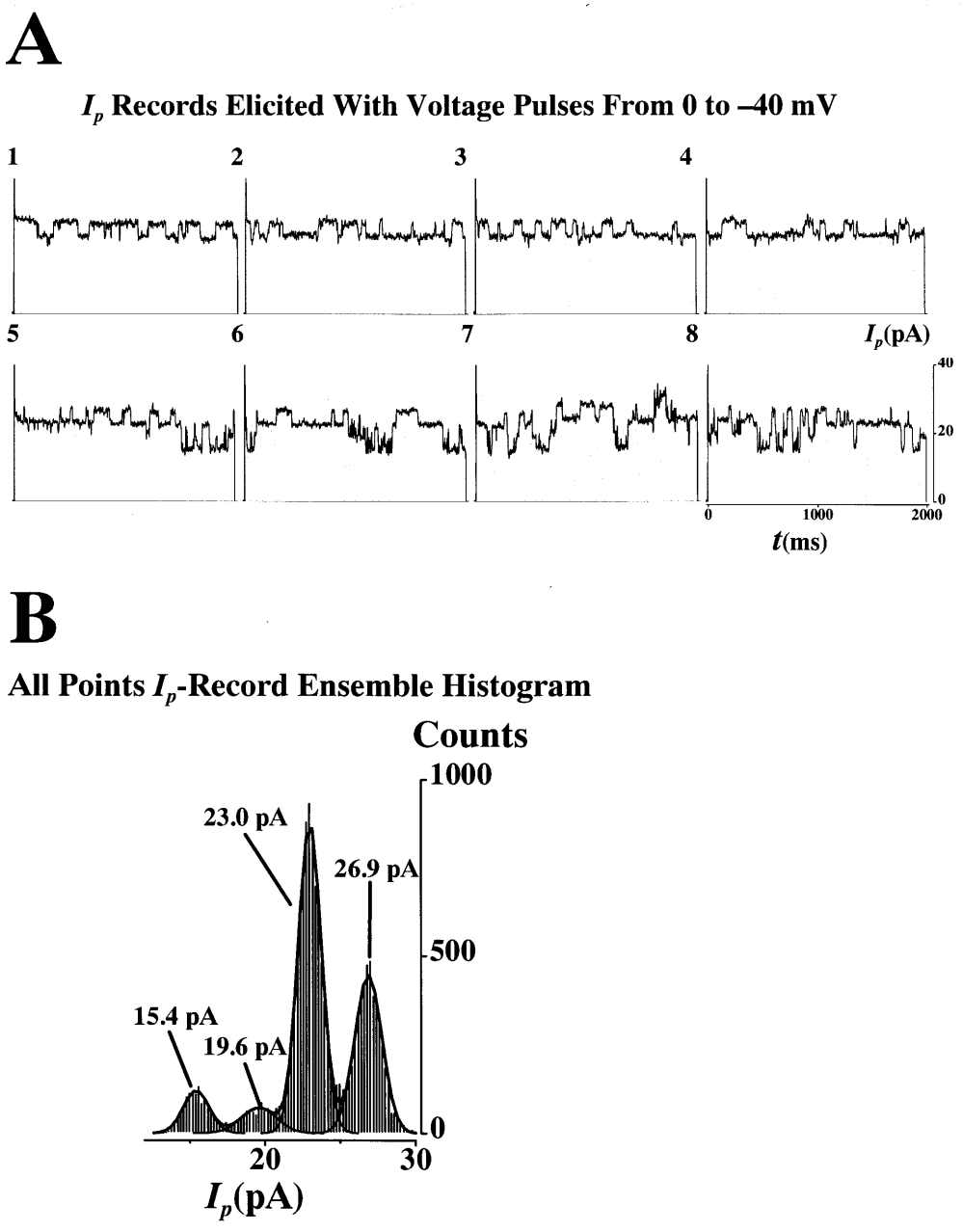

Fig. 1A,B Patch current record ensemble and amplitude histogram. Both direct and indirect methods were use to calculate single nuclear pore complex (*NPC*) ion conductance, γ. **A** Open-close and close-open state transitions were detected by visual inspection of each current, I_p, record in the ensemble consisting of 8 records. The ion current flowing through a single NPC channel was manually measured by calculating the difference between consecutive open-close and close-open channel levels, Δi. The value of γ was the value of Δi divided by the pulse voltage. The number at the top-left of each record shows the sequence order (i.e., 1 for the 1st record, 8 for the 8th). **B** When direct visual identification of the state transitions was not possible due to excessive intrinsic channel noise or slow variations uncharacteristic of ion channels, the all-points amplitude histogram was used with the assistance of multiple Gaussian fitting as shown by the continuous black lines forming the envelope of the whole histogram and of individual Gaussian curves

system consisting of 1 mM MgATP, 5 mM creatine phosphate ditris salt, and 20 units/ml creatine phosphokinase VI-S (Sigma). Cell lysates were prepared by ice-cold centrifugation of the minced tissue (see Nuclei isolation) through a 10,000 mol. wt. microcentrifuge filter (Ultrafree, Millipore, Bedford, Mass., USA). The functional capacity of the nuclear machinery for transcription, RNA export and translation was tested with the EGFP plasmid (pEGFP-C1 ≈3.1 MDa, Clontech Labs, Palo Alto, Calif., USA) containing the 72-base-pair SV40 enhancer in its sequence. The experiments with pEGFP-C1 also were carried out with the enriched lysate. The presence of the SV40 enhancer targeted the plasmid to the nucleus via the transcription factors that attached to it [25, 26]. The long phase lag (3–6 h) between the import of plasmid and the EGFP expression allowed the dissection of import and export events after pEGFP application and support the time course for such events in intact cells [25, 26].

General

All experiments were carried out at room temperature (22–26°C). Basic statistics for the parameters measured are given as mean ±SD along with the number of observations, *n*. (not to be confused with *N*, the number of ion-conducting NPCCs). The number of records inspected is included to provide an indirect means of evaluating the probabilities of finding channel openings.

Results

Fluorescence microscopy of passive and active transport properties

Figure 2 shows the transport properties of the nuclei isolated from adult cardiac myocytes. In all cases, the

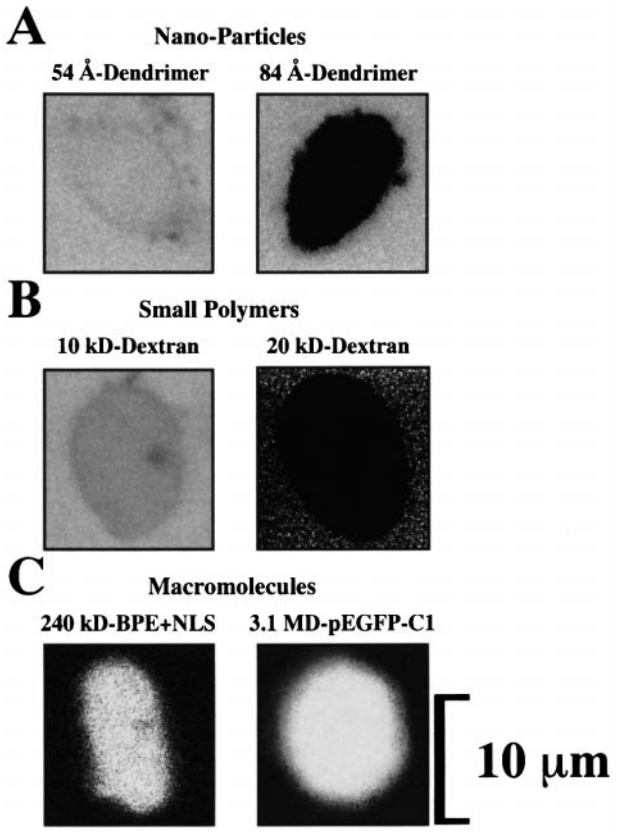

Fig. 2A–C Fluorescence microscopy analysis of the transport properties of isolated adult cardiomyocyte nuclei. **A** NPC sieving properties were studied with FITC-labeled dendrimers of 5.4 nm and 8.4 nm (54 and 84 Å) diameter. All nuclei allowed the entry of 5.4-nm diameter (54 Å) and almost all excluded the 8.4-nm-diameter (84 Å) dendrimer. **B** NPC sieving properties were also studied with conventional FITC-labeled dextrans of 4–150 kDa. The cut-off point for sieving was near 20 kDa as most nuclei excluded this probe. **C** Macromolecular import and transcriptional-translational capacity of the nuclei were tested with nuclear-targeted B-phycoerythrin (*BPE+NLS*) and with the plasmid for enhanced green fluorescence protein *pEGFP-C1*. The light detected from nuclei incubated with pEGFP-C1 comes from the expressed pEGFP product, EGFP. All probes were applied to the nuclear bath and were left throughout the imaging, as this did not interfere with the observation. Some images (e.g., 20 kDa dextran, **B**) are noisy due to the high gain of the photomultiplier required to detect the signal without increasing the intensity of the laser beam, which would otherwise harm the preparation

probes were applied to the nuclear bath and left throughout the imaging, as this did not interfere with the measurement. Some of the images (e.g., 20-kDa dextran, panel B) are noisy due to the high gain of the photomultiplier required to detect the signal without increasing the intensity of the laser beam (which would have deleterious effects on the nucleus). Figure 2A demonstrates that the 5.4-nm-diamter (54 Å) dendrimer particles diffused into the nuclear interior whereas the 8.4-nm-diamter (84 Å) particles did not. However, of the total 78 nuclei observed from the 12 mice studied, we could detect 11 nuclei that did allow the passage of the 8.4-nm-diameter (84 Å) dendrimer into the nuclear interior (15 min observation). This suggests that the NPCC diameter is around 8.4 nm (84 Å). Figure 2B shows that while the 10-kDa dextran particles did go into the nuclei, the 20-kDa dextran particles did not. Again, we observed that of the 12 mice used for FITC-dextran imaging (the same donors as for the dendrimer observations), 16 out of 92 nuclei allowed the entry of 20-kDa dextran particles (15 min observation). This suggests that the limiting molecular weight for this class of polymers must be around 20 kDa. Finally, Fig. 2C demonstrates that these nuclei are capable of importing nuclear-targeted macromolecules. Both BPE+NLS and pEGFP-C1 containing the SV40 enhancer (which allows nuclear import of the plasmid due to transcription factor binding – see [25, 26]) were able to cross the NE in the presence of enriched cell lysate (see Materials and methods). Of all the mice studied, only 4 out of the 67 nuclei did not translocate BPE+NLS (up to 30 min observation) and only 5 of 48 nuclei did not express pEGFP (up to 24 h observation). Since the light recorded from the nuclei treated with pEGFP-C1 derives from the protein product of pEGFP (i.e., EGFP), the image in Fig. 2C also shows that these nuclei are capable of transcribing the nuclear-targeted pEGFP, of exporting the corresponding ribonucleoprotein particles or RNPs (see [21]), and of translating the mRNA molecules encoding for EGFP. As previously observed [6], in the presence of NLS-coupled BPE the single NPCC and patch ion currents (i and I_p, respectively – and thus γ and Γ_p) are reduced to non-detectable levels (not shown). The same effect was seen after incubation with pEGFP-C1 (not shown). In our study it was impossible to reverse these effects within the experimental time. This was probably due to the lack of some transport substrate and/or the excess of cargo.

Patch-clamp studies of colloidal gold and dendrimer particles

Under control conditions (i.e., no nanoparticle added), the value of γ was 396±83 pS (obtained from 96 state transitions from 96 records, 4 patches, 4 mice – see Fig. 1). This value is in agreement with our previously reported control values for this preparation (e.g., 421± 46 pS, n=451, in [6]). The control ion channel activity was very stable, lasted more than 24 h, it did not show openings with reduced γ and had negligible noise (note that the signal-to-noise ratio for the NPCC is very high due to the large value of γ under control conditions; see also [6, 8, 19]). An unexpected effect of colloidal gold was a substantial increase in the noise of the recordings, followed by unstable and leaky seals leading to the loss of the pipette-membrane seal (i.e., the gigaseal, essential for patch-clamp). This effect was unexpected as we are able to maintain this preparation for more than 72 h (e.g., [6, 20]). The effect was clearly due, therefore, to the presence of colloidal gold. This effect seemed to depend on the diameter of the colloidal gold particle. For 20-nm-diameter particles, a concentration $>10^{10}$ particles/l

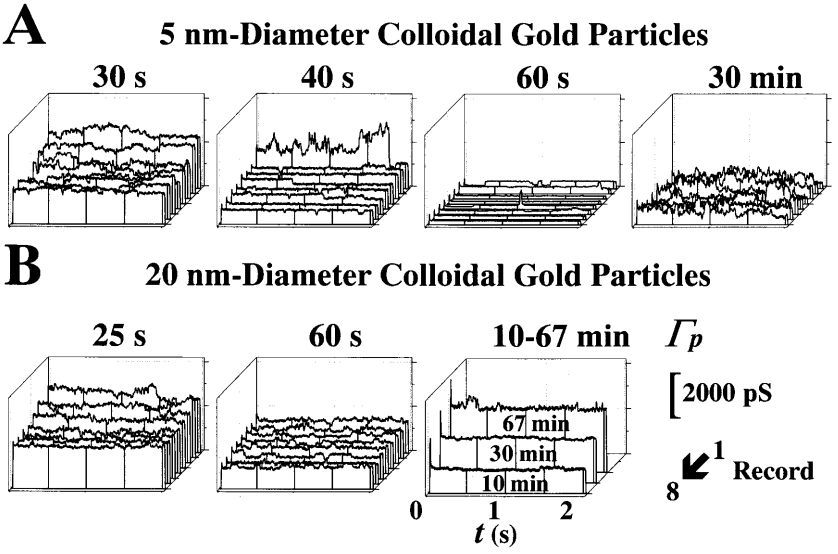

Fig. 3A,B Modification of NPC gating by colloidal gold particles. **A, B** Effects of 5- and 20-nm diameter particles, respectively. Time sequences of the effects of colloidal gold on the eight-record ensembles of patch ion conductance, Γ_p. The records in each ensemble were elicited consecutively, leaving a 300-ms interval during which the nuclear envelope (*NE*) was held at 0 mV. The time of acquisition (following gigaseal formation) of each ensemble is shown at the *top* of each *panel*. Note that Γ_p is the patch current (I_p), normalized by the applied voltage. Therefore, both Γ_p and I_p result from the contributions of all the ion-conducting channels present in the patch (the remainder are presumably plugged by translocating macromolecules). The concentration was estimated at 10^{11} and 10^5 particles/l for 5- and 20-nm diameter particles, respectively. Higher concentrations caused unstable recordings and damaged the nuclear pore, as suggested by the noisy recordings similar to those made at 30 min in **A**. Conductance and time calibrations are shown at the *bottom-right corner*

caused the seal between the pipette and the NE to be lost within a minute (8 patches, 5 mice). At $\cong 10^7$–10^9 particles/l, the seal was maintained for up to 10 min (12 patches, 5 mice) and at $\cong 10^5$ particles/l the seal lasted for up to 1 h (3 patches, 2 mice). For smaller diameter particles, however, the preparations survived considerably longer times at the same concentrations. For example, for 5-nm-diameter particles at 10^{11} particles/l could last 30 min. The colloidal gold particles behaved as if they were poor electrical conductors since the NPCC conductance, γ, transiently decreased with exposure to the particles. This transient decrease was followed by a moderate increase in γ. As explained in Materials and methods, these relatively slow transients, uncharacteristic of typical ion channels, were excluded from the basic single channel statistics as they suggested partial NPCC plugging. The 63 step-like state transitions detected by direct inspection or with the help of the amplitude histogram, yielded a γ=262±81 pS (21 patches, 7 mice; 1512 records individually inspected).

Figure 3 illustrates the effect of colloidal gold particles. Panels A and B show, respectively, the effects of 5- and 20-nm diameter colloidal gold particles on patch ion conductance, Γ_p. The concentration was estimated at 10^{11} and 10^5 particles/liter for the 5- and 20-nm diameter particles, respectively. In Fig. 3A, the ensembles recorded at 30 and 40 s show the early reduction in Γ_p following gigaseal formation. At 40 s the single-channel conductance, γ, can be better appreciated by direct inspection of the records. The reduction in Γ_p, observed at 60 s, was slowly reversed with time, as demonstrated by the ensemble recorded at 30 min. It was interesting to find out that this noisy recording was not the result of a loss in the pipette-envelope seal resistance since we observed a gigaseal of ≈5 GΩ. That is, the noise was intrinsic to the ion channel activity and, therefore, caused by the colloidal gold. Thus, determination of single ion channel properties (e.g., γ and p_o) were rather difficult with conventional statistics (see Materials and methods) since it was unreliable to determine the open and close channel levels even during direct inspection of each record. The value of γ obtained from 30 transitions was 294±65 pS (30 records, 8 patches, 2 mice; 752 records inspected). In Fig. 3B, the ensembles recorded at 25 and 60 s show the initial decrease in the Γ_p that took effect within 1 min of application of 20-nm-diameter colloidal gold particles. At 60 s, a small ion-channel-like activity with brief, step-like openings typical of cell surface ion channels was observed. The on-off gating was followed by a continuous increase in Γ_p without apparent on-off gating. The seal between the pipette tip and the nuclear membrane was then lost. The γ value obtained from 33 state transitions was 233±84 pS (33 records, 12 patches, 5 mice; 760 records inspected).

Dendrimer concentrations causing appreciable effects were $\cong 10^9$ particles/l. Higher concentrations gave unstable recordings similar to the noisy recordings described above for colloidal gold particles. In contrast to the experience with colloidal gold particles, dendrimer particles at these effective concentrations allow very stable preparations, all capable of lasting more than 24 h. A total of 22 patches were investigated in 11 mice (some mice were used for various control and dendrimer tests). From these patches, we inspected each of the 2608 records accumulated.

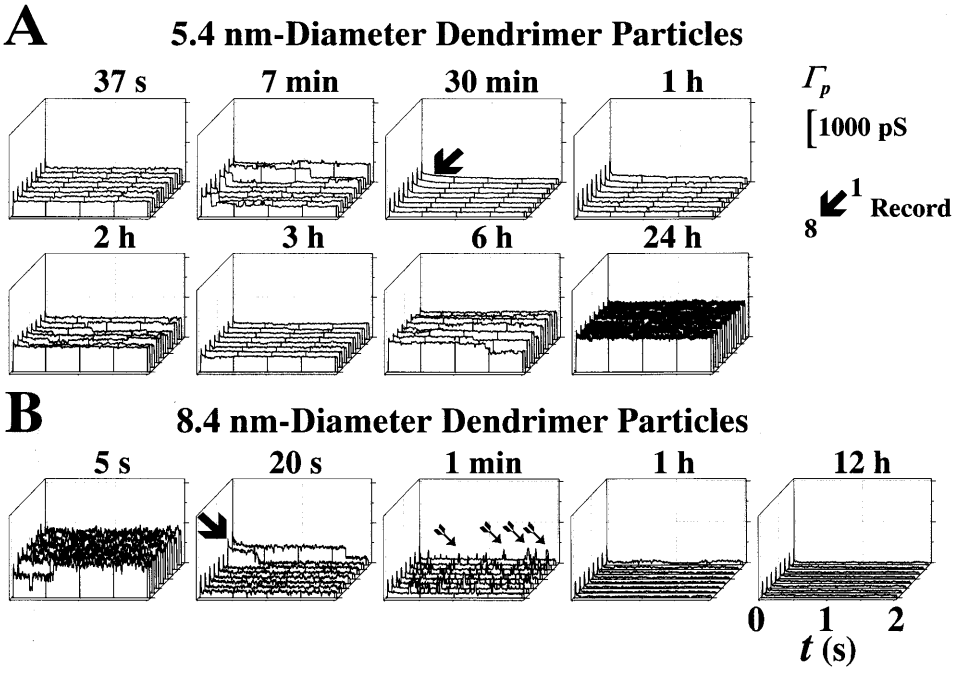

Fig. 4A,B Transient plugging by 5.4- and 8.4-nm diameter dendrimer particles. **A, B** Effects of 5.4- and 8.4-nm diameter dendrimer particles, respectively. Γ_p record ensembles similar to those in Fig. 3. The time of acquisition for each record ensemble is shown at the *top* of each *panel*. The concentration for both 5.4- and 8.4-nm diameter particles was estimated at 10^9 particles/l. **A** The arrow in the ensemble recorded at 30 min indicates a slow transition probably resulting from dendrimer particle translocation through the NPCC. **B** The *arrow* shown at 20 s indicates the moment when the dendrimer particle plugged the NPCC. The *arrows* in the ensemble recorded at 1 min point to brief spikes of ion fluxes probably related to escape of ions through orifices between the dendrimer particles and the lining of the pore lumen. These orifices, however, were short-lived since the pore remained shut, and did not open after a 4-min exposure to the dendrimer particles. Conductance and time calibrations are shown at the *top*- and *bottom-right corners*, respectively

Figure 4 illustrates the effects of 5.4- and 8.4-nm-diameter dendrimer particles. The stability of the preparation in the presence of dendrimers was conspicuous, as illustrated in Fig. 4. Indeed, the experiment shown in Fig. 4A was stopped at will after 40 h of continuous recording. The downward arrow in Fig. 4A (30 min ensemble) points to a slow decrease in γ that was detected after 30 min of recording. This suggests that the particles moved along the NPC aqueous channel, NPCC, to reduce its effective conductivity (i.e., a sort of conductance per unit volume which characterizes the medium). This effect was similar to that reported for transcription factors [6]. Although the transient decrease in γ and Γ_p (N was reduced to zero during total plugging) in Fig. 4A lasted for about 40 min, we observed shorter transients (e.g., lasting only a few seconds) with 5.4-nm-diameter dendrimer particles. We considered this variability to result from the variability in the NPCC diameter (i.e., the longer the plugged time, the smaller the NPCC diameter). The single NPCC ion conductance, γ, obtained from 23 state transitions was 257±22 pS (23 records, 3 patches, 3 mice; 920 records inspected). Figure 4B illustrates the effects of 8.4-nm-diameter particles. The effects were striking. Once the dendrimer particle plugged the channel, no unplugging occurred. The ensemble recorded at 20 s illustrates the instant of pore plugging (second trace indicated with the downward arrow). Incomplete plugging of the pore appeared to allow crevices through which monoatomic ions (mainly K^+ in this preparation, *see* [8, 19]) could penetrate, thus resulting in brief current or conductance spikes (indicated with arrows in the ensemble recorded at 1 min). After these early events, the NPCCs remained completely plugged for the duration of the experiments (22 h in the example of Fig. 4B). The γ value for this experimental series was obtained from 30 state transitions (28 records, 17 patches, 8 mice; 1,480 records inspected).

Discussion

We proposed that the large-γ channel activity recorded with patch-clamp from the NE of cardiac myocytes corresponds to ion flow through the NPC (e.g., [6, 20, 21]; reviewed in [4]). Our fluorescence microscopy data confirm that our preparation is capable of both active macromolecular and passive (diffusional) transport along the NPCC. Given sufficient time, cardiomyocyte nuclei allow the translocation of particles much larger than monoatomic ions (i.e., dextrans and dendrimers). They also allow the translocation of nuclear-targeted macromolecules (i.e., 240 kDa BPE+NLS and 3.1 MDa pEGFP-C1). Furthermore, our experiments with pEGFP-C1 show that our preparation is capable of transcription and translation when given the proper substrates (i.e., enriched cell lysate). These observations confirm that our

preparation contains NPCs that are intact, albeit modified by the bath composition. The study of passive diffusion, by its own definition, does not require any MMT substrate such as ATP. Therefore, the absence of MMT substrates for the tests of dextrans, dendrimers and colloidal gold is immaterial. It is however important to note that Ca^{2+} concentration inside the NE cisterna is an important determinant even for passive diffusion (e.g., [27, 28, 29, 30, 31]; discussed in [21]). Thus, this is a parameter that has to be considered in the determination of the limit for passive diffusion (i.e., NPCC passive diameter). Our fluorescence microscopy data, therefore, demonstrate that the NPC population in our preparation remained functional. Thus, any potential ER contribution to patch-clamp recordings, as proposed in [23], must be minimal in our preparation (reviewed in [4]).

Since colloidal gold particles are commonly used with EM to assess the NPC diameter, we used colloidal gold with patch-clamp, under the model of macromolecule-conducting ion channels (see [4, 6]). Much to our surprise, we found that colloidal gold particles modify both the NPC gating and the NE stability of our isolated adult cardiac myocyte nuclei. Colloidal gold particles are manufactured from hydrogen tetrachloroaurate ($HAuCl_4$), a substance known to be corrosive, caustic, hygroscopic and light-sensitive (Merck Index). Due to the high dilution used ($<10^{12}$ particles per liter), and the extreme caution followed in preparing the solutions in these investigations (see Materials and methods), we think that the effects were not due to impurities (e.g., traces of $HAuCl_4$ molecules not forming colloidal particles). Furthermore, these effects of 20-nm-diameter colloidal gold were seen with two different batches of the commercial product. Our results from isolated cardiac myocyte nuclei suggest that colloidal gold may lead to artifactual estimates of NPCC diameter in this and other preparations.

The apparent dielectric-like behavior of the colloidal gold particles may be related to their unavailability to serve as charge carriers and/or their ability to alter pore gating. It is interesting to note that while the dendrimer particles of 8.4 nm diameter plugged the pores, the 20-nm-diameter colloidal gold particles appeared to allow ion conduction. This may be a result of imperfect colloidal gold or of the colloidal gold-induced modifications of the NPCs. The nature of the small γ channel activity observed with 20-nm-diameter colloidal gold particles is interesting, but at this moment difficult to explain with certainty. The fluorescence microscopy observations with FITC-labeled dendrimers support the idea that the NPCC diameter is around 8.4 nm diameter because most of the nuclei excluded the probe. Thus, the experiments with calibrated dendrimer particles demonstrate the suitability of this material to measure with patch-clamp the NPCC diameter.

Another interesting phenomenon was observed with all dendrimers studied but mostly (≈70% of the time) during experiments with 8.4-nm-diameter dendrimer particles: the Γ_p and γ spikes. We interpret these spikes as result of monoatomic ion movement through crevices left open during the short-lived process of dendrimer interaction with the NPCC during plugging. If this interpretation is correct, then the spiking seen with smaller diameter particles indicates that the NPCC was reduced in its effective functional diameter (i.e., not necessarily that corresponding to a perfect circular cylinder). Note that the full amplitude of the spikes is below the actual values due to the 100 Hz filter used for our signals in our experiments (see Materials and methods). We think, however, that the short-lived spiking phenomenon may be helpful in understanding the mechanisms of gating not only in NPCCs but in other types of macromolecule-conducting channels and ion channels in general.

We have shown here that patch-clamp can be used with calibrated dendrimers to rapidly assess the NPCC sieving diameter. Our patch-clamp estimate of the NPCC diameter, 8–9 nm, falls within the range of values reported for the NPC channel of *Xenopus laevis* oocytes (reviewed in [2, 3, 4]). Therefore, the patch-clamp approach for assessing NPCC functional diameter seems advantageous. Our studies with high-resolution field emission scanning EM (FESEM; J.O. Bustamante, unpublished observations) suggest that small variations in pore diameter are to be expected. The present report also shows that, despite its relatively large diameter, the unplugged NPCC is capable of restricting monoatomic ion flow in an open-close probabilistic manner (see [19]). Our approach to evaluating the functional NPC channel diameter should be useful in determining changes associated with various physiological (e.g., cell cycle phase) and pathological conditions (e.g., immune response, cancer).

Acknowledgements We would like to thank Dr. Alan Finkel (Axon Instruments) for assistance with the data acquisition instrumentation and Dr. Rosaria Haugland (Molecular Probes) for assistance with some fluorescent probes. We are greatly indebted to Joe Sanguedulce, Mike Hernandez, and Harrison L. Weese of Nissei Sangyo America, for their assistance with their high-resolution FESEM instrumentation. This work was partly supported by the Medical Research Council (MRC) of Canada, by the American Heart Association (AHA), and by the Fundação de Apoio à Pesquisa do Estado de São Paulo (FAPESP) to J.O.B. and by NIH to J.P.G., T.J.M. and D.A.D.

Appendix I

Analysis of effects of translocating non-charge carriers on NPC ion conductance, γ

The analysis of the effects caused by particles that completely plug the NPCC is relatively easy, as plugging implies stopping the ion flow. In this case, the NPCC ion conductance, γ, is zero because there is no current (i.e., Δi or i heretofore is 0), and by definition, $\gamma = i/V$ (where V is the voltage gradient between the nuclear and cytoplasmic faces of the NPCC – which we will assume independent of the translocating ions and other particles). However, when relatively large particles (e.g., dendrimers) that cannot carry electrical charges are introduced in the medium, γ is reduced because the number of available charge carriers (e.g., K^+) is reduced. Under these circumstances, one can make a simple first-order analysis of the changes caused by such a situation. In our analysis let us ignore the effects of hydration on the basis of the large pore diameter and the relatively inert nature of the particles. Since i is

the rate of change of electrical charges, q, (i.e., $i=dq/dt$; with t representing time), we have $\gamma=dq/dt/V$. The relationship between full and reduced γ, γ_{full} and $\gamma_{reduced}$, respectively, is simply $\gamma_{full}/\gamma_{reduced}=dq_{full}/dq_{reduced}$.

The amount of electrical charge, dq_{full}, in the fully available volume, v_{full}, is the concentration of charges, $[K^+]$ in our case, times v_{full}: $dq_{full}=[K^+]v_{full}$. Likewise, the amount of charges, $dq_{reduced}$, in the reduced unit volume, $v_{reduced}$, is the $[K^+]$ times $v_{reduced}$: $dq_{reduced}=[K^+]v_{reduced}$. The reduced volume equals the full volume minus the volume taken up by the particles that are not electrical charge carriers.

$$v_{reduced}=v_{full}-\xi(\eta v_{full})=v_{full}(1-\xi\eta)$$

where η is the concentration of particles which are not electrical charge carriers and ξ is the volume of individual particles (e.g., if the diameter of the particles is d, then $4/3\pi(d/2)^3$, or $\pi d^3/6$.

$$\gamma_{full}/\gamma_{reduced}=dq_{full}/dq_{reduced}=[K^+]v_{full}/[K^+]v_{reduced}=1/(1-\xi\eta)$$

$$\gamma_{full}/\gamma_{reduced}=1/(1\xi\eta)$$

or

$$\gamma_{reduced}=(1-\xi\eta)\gamma_{full}$$

References

1. Feldherr CM (1986) The use of electron-opaque tracers in nuclear transport studies. In: Peters R, Trendelenburg M (eds) Nucleocytoplasmic transport. Springer-Verlag, Berlin, pp 53–61
2. Miller M, Park MK, Hanover JA (1991) Nuclear pore complex: structure, function and regulation. Physiol Rev 71:681–686
3. Stoffler D, Fahrenkrog B, Aebi U (1999) The nuclear pore complex: from molecular architecture to functional dynamics. Curr Opin Cell Biol 11:391–401
4. Bustamante JO, Varanda WA (1998) Patch-clamp detection of macromolecular translocation along nuclear pores. Braz J Med Biol Res 31:333–354
5. Nigg EA (1999) Transport across the nuclear membrane. Nature Cell Biol 1:195–197
6. Bustamante JO, Hanover JA, Liepins A (1995) The nuclear pore ion channel activity. J Membr Biol 146:239–251
7. Tonini R, Grohovaz F, Laporta CA, Mazzanti M (1999) Gating mechanism of the nuclear pore complex channel in isolated neonatal and adult mouse liver nuclei. FASEB J 13:1395–1403
8. Bustamante JO (1992) Nuclear ion channels in cardiac myocytes. Pflügers Arch 421:473–485
9. Simon SM, Blobel G (1991) A protein-conducting channel in the endoplasmic reticulum. Cell 65:371–380
10. Bezrukov SM, Vodyanoy I, Parsegian VA (1994) Counting polymers moving through a single ion channel. Nature 370:279–281
11. Kasianowicz JJ, Brandin E, Branton E, Deamer DW (1996) Characterization of individual polynucleotide molecules using a membrane channel. Proc Natl Acad Sci USA 93:13770–13773
12. Badminton MN, Kendall JM, Rembold CM, Campbell AK (1998) Current evidence suggests independent regulation of nuclear calcium. Cell Calcium 23:79–86
13. Lohret TA, Kinnally KW (1995) Targeting peptides transiently block a mitochondrial channel. J Biol Chem 270:15950–15953
14. Henry JP, Juin P, Vallette F, Thieffry M (1996) Characterization and function of the mitochondrial outer membrane peptide-sensitive channel. J Bioenerg Biomembr 28:101–108
15. Szabò I, Bàthori G, Tombola F, Coppola A, Schmehl I, Brini M, Ghazi A, De Pinto V, Zoratti M (1998) Double-stranded DNA can be translocated across a planar membrane containing purified mitochondrial porin. FASEB J 12:495–502
16. Peters R (1986. Fluorescence microphotolysis to measure nucleocytoplasmic transport and intracellular mobility. Biochim Biophys Acta 864:305–359
17. Keminer O, Peters R (1999) Permeability of single nuclear pores. Biophys J 77:217–228
18. Keminer O, Siebrasse JP, Zerf K, Peters R (1999) Optical recording of signal-mediated protein transport through single nuclear pore complexes. Proc Natl Acad Sci USA 96:11842–11847
19. Bustamante JO (1993) Restricted ion flow at the nuclear envelope of cardiac myocytes. Biophys J 64:1735–1749
20. Bustamante JO, Oberleithner H, Hanover JA, Liepins A (1995) Patch-clamp detection of transcription factor translocation across nuclear pores. J Membr Biol 146:253–261
21. Bustamante JO, Michelette ERF, Geibel JP, Dean DA, Hanover JA, McDonnell TJ (1999) Calcium, ATP, and nuclear pore channel gating. Pflügers Arch (in press)
22. Tomalia DA (1995) Dendrimer molecules. Sci Am 272:62–66
23. Danker T, Mazzanti M, Tonini R, Rakowska A, Oberleithner H (1997) Using atomic force microscopy to investigate patch-clamped nuclear membrane. Cell Biol Int 21:747–757
24. Bustamante JO (1991) An inexpensive inverted microscope for patch-clamp and other electrophysiological studies at the cellular level. Pflügers Arch 418:608–610
25. Dean DA (1997) Import of plasmid DNA into the nucleus is sequence-specific. Exp Cell Res 230:293–302
26. Dean DA, Dean BS, Muller S, Smith LC (1999) Sequence requirements for plasmid nuclear import. Exp Cell Res 253:713–722
27. Stehno-Bittel L, Perez-Terzic C, Clapham DE (1995) Diffusion across the nuclear envelope inhibited by depletion of the nuclear Ca^{2+} store. Science 270:1835–1838
28. Pérez-Terzic C, Pyle J, Jaconi M, Stehno-Bittel L, Clapham DE (1996) Conformational states of the nuclear pore complex induced by depletion of nuclear Ca^{2+} stores. Science 273:1875–1877
29. Lee MA, Dunn RC, Clapham DE, Stehno-Bittel L (1998) Calcium regulation of nuclear pore permeability. Cell Calcium 23:91–101
30. Petersen OH, Gerasimenko OV, Gerasimenko JV, Mogami H, Tepikin AV (1998) The calcium store in the nuclear envelope. Cell Calcium 23:87–90
31. Stoffler D, Goldie KN, Feja B, Aebi U (1999) Calcium-mediated structural changes of native nuclear pore complexes monitored by time-lapse atomic force microscopy. J Mol Biol 287:741–752